

Test-rig design for automated evaluation of automotive electro-chemical sensors

Master's thesis in Embedded Electronic System Design

SHILPA GUPTA

MASTER'S THESIS 2020

Test-rig design for automated evaluation of automotive electro-chemical sensors

SHILPA GUPTA



UNIVERSITY OF
GOTHENBURG



CHALMERS
UNIVERSITY OF TECHNOLOGY

Department of Computer Science and Engineering
CHALMERS UNIVERSITY OF TECHNOLOGY
UNIVERSITY OF GOTHENBURG
Gothenburg, Sweden 2020

Test-rig design for automated evaluation of automotive electro-chemical sensors
SHILPA GUPTA

© SHILPA GUPTA, 2020.

Supervisor: Sr. Lect. Lars Svensson, Dept. of Computer Science and Engineering
Advisor: Mr. Ghassan Alrheis, Dr. Peter Linqvist & Prof. Ola Stenlåås, Scania CV
AB
Examiner: Prof. Per Larsson-Edefors, Dept. of Computer Science and Engineering

Master's Thesis 2020
Department of Computer Science and Engineering
Chalmers University of Technology and University of Gothenburg
SE-412 96 Gothenburg
Telephone +46 31 772 1000

Cover: Bench testing of NO_x sensors and other test components

Typeset in L^AT_EX
Gothenburg, Sweden 2020

Test-rig design for automated evaluation of automotive electro-chemical sensors
SHILPA GUPTA
Department of Computer Science and Engineering
Chalmers University of Technology and University of Gothenburg

Abstract

The main aim of this project is the design and development of an automated test-rig for testing automotive electro-chemical sensors. The main targeted sensor is NO_x (Compounds of Nitrogen oxide), which is one of the most critical and failure-prone components of exhaust after-treatment system. Based on the gas concentration measurements from these sensors, several actions are taken to reduce the vehicle emissions and comply with required emission guidelines by government. An automated test-rig can perform various combinations of temperature and gas variations on multiple sensors simultaneously while reducing the operating test time compared to manual one. Added to the advantage is the scope of detailed analysis of faulty field sensors thereby increasing the overall productivity.

A cRIO (Compact Re-configurable Input Output) is used as the main embedded controller to carry out test command and control, data logging and saving, and communication with sensors and other test-rig hardware components. The test software is developed in LabVIEW (Laboratory Virtual Instrument Engineering Workbench). To reduce operating complexity, script-based command files are made to control various test-rig equipment. Finally, a GUI (Graphical User Interface) is developed for user interaction and real-time monitoring during on-going test.

A working automated test-rig is successfully developed and its performance is compared to manual operation through a series of tests. The final testing was carried out in a test cell (gas-sealed box) with provision to mount sensors and other accessories like gas inlet/ outlet valves, gas flow controller and pressure sensor. Several test cases were conducted to evaluate three NO_x sensors in three different gas environment - air, nitrogen and NO_x (489 ppm concentration). The sensors under test corresponded well to the gas variations resulting in NO_x and O₂ measurements within the expected range of ≈ 467 ppm and 20 % respectively.

The aim of the project is successfully met with around 50 % of active operator/ operating time saved by automated test-rig over manual one. In addition, this test-rig removes the intermittent delays of manual maneuvers resulting in better repeatability performance. Due to limitation of resources, some features and test cases could not be incorporated and their implications are further discussed. As a further improvement, additional safety features can be added and the test-rig can be extended for testing other types of sensors.

Keywords: Automotive sensors, Test automation, NO_x, Test-rig, cRIO, LabVIEW

Acknowledgements

Having worked with hardware aspects of projects for better part of my professional journey, I had natural inclination towards them. However, I always felt that I needed to improve myself in software field. This thesis came as a dream come true. A perfect combination of hardware and software development, its all I could have asked for. I got to learn new tools & skills, work in a amiable professional environment at Scania CV AB and gain from the guidance of four amazing mentors.

This thesis wouldn't have been possible without Ola Stenlåås, one of my Scania supervisors. I would like to thank Ola for believing in me and taking initiative for conception of this thesis based on my area of interest. He not only managed all the administrative part of thesis but also gave valuable feedback through out all aspects of the project.

I would like to thank Peter Linqvist, my another Scania supervisor, for his guidance towards the hardware part of the project. Peter had a clear vision of what is required in the project and helped me in understanding & visualizing the project better. From ordering components to actual testing, he always ensured that I had the required hardware to carry out my work.

The software accomplishments in this project wouldn't have been possible without Ghassan Alrheis, my third Scania supervisor. I was a newbie with LabVIEW tool, yet I had the courage to take up the entire software development in this project because I knew he had my back. Whenever, wherever and however I was stuck, he was always there to help. He was more like a friend than a supervisor to me.

Next, I would like to thank Lars Svensson, my Chalmers supervisor for his constant support. Lars was not only the academic supervisor but my teacher and mentor. In this project, he gave me wings to explore new horizons as well as kept me rooted to maintain high academic levels. I would always be grateful for his understanding and motivation towards various obstacles I faced during this thesis.

I would like to thank Jonas Holmborn, my manager at Scania who was always appreciative for all the work. Jonas was the one who got me into Scania through Scania Student Intro program and I thank him for this wonderful opportunity. I would also like to thank my examiner Per Larsson-Edefors for his patience and quick feedback. To meet his vision towards thesis's academic levels, was like a driving force for me.

Last but not the least, I would like to thank friends and family, especially my parents for their trust and support. This thesis gave me opportunity to upgrade my skills, overcome unforeseen challenges (like COVID-19) and finally evolve myself as a better professional.

Shilpa Gupta, Gothenburg, October 2020

Contents

Abbreviations	xi
List of Figures	xiii
List of Tables	xv
1 Introduction	1
1.1 Background study	1
1.2 Problem statement	3
1.3 Approach	3
1.4 Delimitations	3
2 Technical Background	5
2.1 Exhaust after-treatment system	5
2.2 Electro-chemical sensor	6
2.2.1 NOx sensor	6
2.2.2 Wide band lambda sensor	7
2.3 CAN interface	8
3 Method	9
3.1 Test-rig hardware components	9
3.1.1 Test cell	9
3.1.2 cRIO	12
3.2 Test-rig software components	12
3.2.1 FPGA configuration	12
3.2.2 CAN interfacing	12
3.2.3 Test script	14
3.3 Test-rig software flow plan	14
3.4 Graphical User Interface (GUI) and Code explanation	16
3.5 Experiment plan	19
4 Results and Discussion	21
4.1 Testing Scenario	21
4.2 Test cases	22
4.2.1 Test case 1	22
4.2.2 Test case 2	25
4.3 Automated test-rig comparison	27

Contents

4.3.1	Operator/ Operating time	28
4.3.2	Repeatability	29
4.4	Other sensor testing	31
5	Conclusion	33
6	Future Works	35
	Bibliography	37

Abbreviations

API - Application Programming Interface
ATI1 - After Treatment Intake bank 1
ATI2 - After Treatment Intake bank 2
ATO1 - After Treatment Outlet bank 1
ATO2 - After Treatment Outlet bank 2
BAM - Broadcast Announce Message
CAN - Controller Area Network
CAN-H - CAN High
CAN-HS/FD - CAN High speed/ Flexible datarate
CAN-L - CAN Low
CAN-LS/FT - CAN Low speed/ Fault tolerant
CE - Conformité Européenne (French for 'European Conformity')
cRIO - Compact Re-configurable Input Output modules
CSMA/CD+AMP - Carrier-Sense, Multiple-Access with Collision Detection and Arbitration on Message Priority
.dbc - DataBase Container file format
DOC - Diesel Oxidation Catalysts
DPE - Dew Point Enable
DPF - Diesel Particulate Filters
ECU - Electronic Control Unit
FET - Field Effect Transistor
FPGA - Field Programmable Gate Array
GUI - Graphical User Interface
HS - Harmonized System
IO - Input/ Output
ISO - International Organization for Standardization
LabVIEW - Laboratory Virtual Instrument Engineering Workbench
NO - Nitric oxide
NO₂ - Nitrogen dioxide
NO_x - Compounds of Nitrogen oxide (mainly NO & NO₂)
OBS - On board System
PEMS - Portable Emissions Measurement System
SCR - Selective Catalytic Reduction
SCU - Sensor Control Unit
SiC - Silicon-Carbide
SoC - System on Chip
STP - Scania Test Platform
VDE - Verband der Elektrotechnik
VI - Virtual Instrument
YSZ - Yttrium stabilized Zirconium oxide

List of Figures

2.1	Selective Catalytic Reduction (SCR) system [15].	5
2.2	Schematic of NOx sensor [16].	6
2.3	NOx sensor.	7
2.4	Wide band lambda sensor.	8
2.5	Extended CAN frame format [18].	8
3.1	Block diagram for test-rig setup.	9
3.2	Hardware pin connections between temperature controller and cRIO.	10
3.3	Hardware pin connections between solenoid valves and cRIO.	10
3.4	Hardware pin connections between pressure sensor and cRIO.	11
3.5	Hardware pin connections between flow controller and cRIO.	11
3.6	Flowchart for CAN interfacing logic.	13
3.7	Example test script.	14
3.8	Overall software flow plan for test-rig.	15
3.9	User input and monitoring GUI	17
3.10	Output GUI	18
4.1	NOx sensors mounted on old test cell.	21
4.2	Final test set up.	22
4.3	NOx measurement for Manual test case. Left y-axis shows NOx values in ppm and right y-axis shows valve position (0=off, 1=on). The sensors NOx measurement increases when NOx valve is on and decreases to 0 for other gases.	23
4.4	O ₂ measurement for Manual test case. Left y-axis shows O ₂ values in % and right y-axis shows valve position (0=off, 1=on). The sensors O ₂ measurement increases when air valve is on and decreases to 0 for other gases (nitrogen and NOx).	24
4.5	NOx measurement for Automatic test case. Left y-axis shows NOx values in ppm and right y-axis shows valve position (0=off, 1=on). The sensors NOx measurement increases when NOx valve is on and decreases to 0 for other gases.	25
4.6	Zoomed in NOx measurement for Automatic test case. Sensor 3 has faster response while sensor 1 measurement is more accurate.	26
4.7	O ₂ measurement for Automatic test case. Left y-axis shows O ₂ values in % and right y-axis shows valve position (0=off, 1=on). The sensors O ₂ measurement increases when air valve is on and decreases to 0 for other gases (nitrogen and NOx).	27

4.8	Valve repeatability test case. Manual testing has more intermittent delays during valves maneuvering compared to automatic one.	30
4.9	Accumulated delays in manual testing for test case in Section 4.3.2. Around 3s of delay is accumulated in manual test over automated for a total test time of 6 min.	31

List of Tables

3.1 cRIO plug-in modules.	12
-----------------------------------	----

1

Introduction

One of the main challenge in today's automotive industry is to provide efficient, economic and comfortable mobility solutions with low environmental impact. To achieve this, sensors and related electronic control units (ECUs) play a crucial role. Since automotive emission is a major contributor to pollution, stricter regulations for emissions are enforced by governments. To comply with these requirements, more reliable and effective exhaust after-treatment solutions are needed. Oxides of Nitrogen (NOx) are an important component of automotive emissions to be reduced and are measured by NOx sensors. As per Euro VI [1] which is the latest emission regulation by European commission, the limits for NOx emissions for heavy duty vehicles is 0.4 g/kWh.

Another critical sensor for exhaust is oxygen or lambda sensor which measures the concentration of oxygen in exhaust gas. This sensor also helps in cross-checking if the after-treatment system is working properly. These electro-chemical sensors are subjected to harsh temperature and chemical conditions in vehicle's tail-pipe resulting to their failure which further leads to increased manufacturing cost. Especially, NOx sensors have a high failure rate and are frequently replaced owing to any discrepancies found in exhaust after-treatment systems. Failure of these sensors also results in reduced performance of exhaust after-treatment systems thereby increasing the emissions. This is more of concern for heavy-duty diesel-run vehicles because compared to gasoline, diesel engine generates more complex emissions. Hence a test solution is required for testing and identifying faulty sensors which is the motivation behind this thesis.

1.1 Background study

Various studies have been conducted to analyze the impact of automotive emissions on environment and human health. J E Jonson et al [2] have studied the adverse effects of excess NOx emissions especially from diesel vehicles across Europe and attributed 80% increase in premature deaths to NOx emissions. As NOx sensors play a significant role in reducing these emissions, several studies have been carried out to analyse their performance, reasons for faulty readings and failure. Various measures are studied to predict and correct NOx sensor errors encompassing from software oriented approach to designing of a new hardware.

Ram B Gurung et al [3] have utilized the operational and environmental data from

heavy-duty trucks by Scania CV AB, to predict NOx sensor breakdown with the help of machine learning algorithms. A common pattern was observed between trucks with faulty and healthy NOx sensors which can be further studied by physical testing of sensors. Ronald R. Yager et al [4] studied the limitations of a physical NOx sensor and a virtual sensor and developed an algorithm which combines their outputs to produce a more relevant NOx reading. Also, the algorithm predicts the fault status of NOx sensors for further replacement.

Apart from complete failure, there are various factors which lead to deviations in NOx sensor readings. Most common are the presence of other chemical compounds in vehicle tail-pipe and temperature variations. Yue Yun Wang et al [5] observed that the presence of ammonia in vehicle's tail-pipe results in higher NOx readings than the actual one. In addition, this mismatch in NOx readings aggravates with increase in temperature. To resolve this issue, an algorithm for NOx reading correction was developed using fuzzy logic. This algorithm identifies a dependence factor of cross-sensitivity of NOx sensor to temperature.

A different approach to counteract the effect of ammonia on NOx sensor readings is by applying a physical filter as seen in the study by Kyongtae Kim et al [6]. It was observed that sensor aging, temperature and presence of humidity further restricts the sensor reading correction. Hence, a gas filter of glass wool, activated charcoal and polymer binder was designed and fabricated. On testing, it was concluded that approximately 71% ammonia can be filtered out based on different gas mixtures.

Several studies [7] [8] [9] have been carried out to improve the design of NOx sensor by experimenting with different chemical compounds; in order to reduce its failure and achieve better results. In [7], a novel NOx sensor was developed based on Silicon Carbide - Field Effect Transistor (SiC-FET). The advantages of semi-conductor technology were utilized for this sensor to achieve NO detection with high sensitivity (< 1 ppm) and high temperature performance along with low size and cost. While, [8] explores a new gadolinium-doped ceria based electrolyte to reduce the effect of other chemical compounds on NOx sensing; [9] experiments with Li_3PO_4 electrolyte to achieve good selectivity.

Owing to the importance of emission detection, various emission measurement systems are developed. Horiba OBS-one [10] is a portable emission measurement system which is widely used by automotive manufacturers to test emission requirements for vehicle certification. A MSc thesis by Jonas Eriksson and Simon Fagerholm [11] was aimed at prototype development of a simplified emission measurement system called PEMSLight (Portable emissions measurement system) and compares the performance to commercially available system. However, these systems target the testing of entire exhaust system of vehicle for emissions, requires customized tail-pipe and has high form factor and cost.

1.2 Problem statement

The frequent failures of above mentioned sensors and their significance in the effective functioning of after-exhaust systems, motivates automotive manufacturers to perform stringent testing of these sensors. However, most of this testing at Scania CV AB, is currently done manually and there is a need to automate the entire test process. Hence, in this thesis an automated test-rig is designed to carry out testing of these field sensors which are already employed on trucks and are suspected to be faulty. The main target sensors for this thesis are NOx and lambda sensors. To imitate the gaseous conditions of a vehicle's tail-pipe, the sensors are tested in three different environments: air, nitrogen and NOx. The main objectives which this thesis aims to find are:

- To quantify the potential of automated test-rig over manual test-rig in terms of operator/ operating time.
- To quantify the test repeatability of automated testing vs manual testing.

1.3 Approach

The main hardware for test-rig are Compact Re-configurable IO modules (cRIO) [12] as main controller and a test cell (gas-sealed box) containing various equipment to provide required test environment for sensors. For programming, LabVIEW [13] is used to control all hardware test equipment and perform testing.

From safety point of view, most of the equipment for the test-rig are chosen for 24 V. The test set up is insulated with an outer grid to avoid human contact owing to high temperatures involved. As the nitrogen gases are toxic in nature, sealing is done against any kind of gas leakage. To ensure that it is safe to perform gas testing at high temperatures, verification checks are conducted within Scania CV AB.

1.4 Delimitations

Based on the data from NOx sensors, a reducing agent (mostly urea and water) is doused in exhaust gases which further converts NOx into nitrogen, water and carbon-dioxide. However, dousing process is out of scope of this project as the main aim is to test the sensors in an automated way. A total number of eight sensors can be tested at a time owing to the limitations of test cell design as well as the maximum number of CAN (Controller Area Network) addresses handled by a port. Most of the equipment and interfaces are remotely controlled except for some gas valves which needs manual control. The testing can be performed for an over-pressure of up to 0.5 bar if the test cell is properly sealed, however for most purposes a small over-pressure is easy to handle. The sensors are planned to be tested only for temperature and gas concentration variation, no other sensor parameters are evaluated due to the complexity involved. Ammonia sensor testing as initially proposed is limited by available resources at Scania CV AB, hence not included as part of this project.

2

Technical Background

The details and functionality of exhaust after-treatment system and components are explained in this chapter.

2.1 Exhaust after-treatment system

To reduce the vehicle emissions and meet global emission guidelines, various after-treatment solutions have been developed like NO_x absorbers and Selective Catalytic Reduction (SCR) system. SCR [14] is currently the most common exhaust after-treatment system for heavy-duty vehicles. In SCR, NO_x sensors are used to measure the NO_x concentration in exhaust gases. Based on the data from NO_x sensor, a reducing agent (mostly urea and water) is doused in exhaust gases as shown in Figure 2.1 [15].

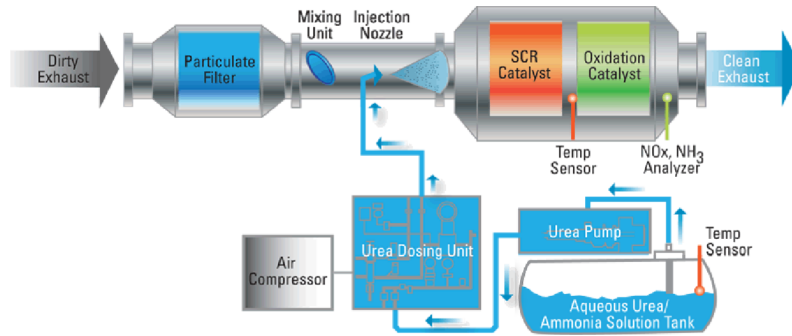
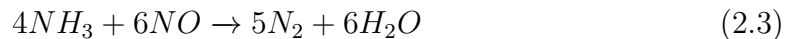
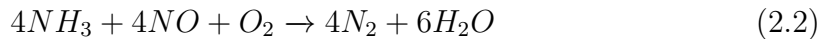


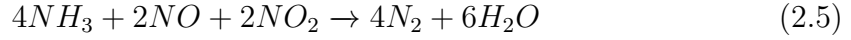
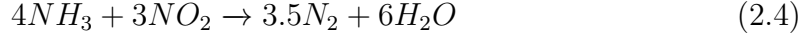
Figure 2.1: Selective Catalytic Reduction (SCR) system [15].

The urea ($\text{CH}_4\text{N}_2\text{O}$) first converts into ammonia (NH_3) due to the high temperature in vehicle tail-pipe by:



The main NO_x compounds in exhaust gases are $\approx 90\%$ NO (Nitric oxide) which is mostly emitted at high temperature and $\approx 5\%$ NO₂ (Nitrogen dioxide) emitted at low temperature [14]. These are further converted to nitrogen, water and carbon-dioxide after reaction with ammonia by:





2.2 Electro-chemical sensor

Electro-chemical sensors are used to measure concentration of a specific gas in terms of electrical signal (mostly current). These sensors consist of electrolyte and electrodes where in a chemical reaction oxidation or reduction occurs due to interaction with gas, resulting in output current. Various types of electro-chemical sensors are used in automotive to measure gases like NOx, oxygen, ammonia, hydrocarbons etc. NOx and lambda are the two most important sensors used in exhaust after-treatment systems; they are also the focus of this thesis.

2.2.1 NOx sensor

NOx sensors measure the concentration of NOx gases in vehicles. In general, two types of NOx sensors are present: upstream and downstream. Both the sensors are mostly similar in terms of working principle, but have different CAN IDs, mechanical connector, mounting location in vehicle's tail-pipe and sometimes measurement range. Upstream NOx sensors namely ATI1 (After Treatment Intake bank 1) and ATI2 (After Treatment Intake bank 2) are mounted before the exhaust after-treatment system while downstream sensors namely ATO1 (After Treatment Outlet bank 1) and ATO2 (After Treatment Outlet bank 2) at the end of tail-pipe.

The NOx sensors used by Scania CV AB are based on Yttrium stabilized Zirconium oxide (YSZ) technology and are internally heated up to 800 °C. A simple NOx sensor consists of two electro-chemical cell - O₂ cell and NO cell as shown in Figure 2.2 [16].

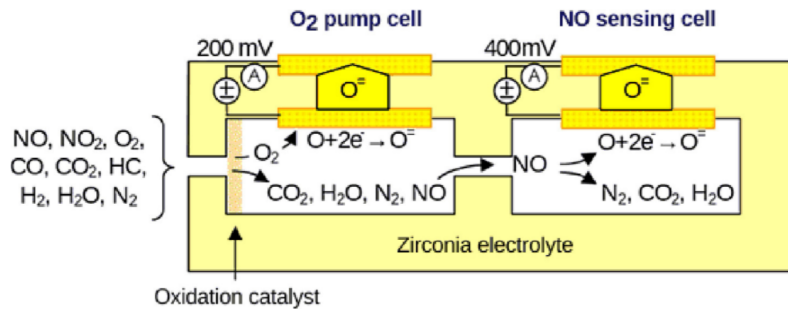


Figure 2.2: Schematic of NOx sensor [16].

The exhaust gas is first passed through the O₂ cell, where all hydrocarbons and O₂ are removed and NO₂ is converted into NO which is passed to the next NO cell. In O₂ cell, O²⁻ ions are formed at electrode surface by:



These O^{2-} ions are pumped through the YSZ electrolyte by applying a fixed low voltage over the pump cell. The ion current is proportional to O_2 level. In NO cell, NO is further chemically converted to nitrogen and oxygen by:



The oxygen (2 O) in this second cell (NO cell) is pumped out in the same way as in the first cell (O_2 cell). Measured NO is proportional to the pumped oxygen in NO cell. A known potential is applied through the zirconia based electrolyte in the cell and the obtained current from first cell gives the oxygen concentration in exhaust gases. The current obtained from second cell is proportional to oxygen concentration from NO and hence indirectly represents NOx concentration.

Figure 2.3 shows a model of the NOx sensor used for testing in this project. It consists of a sensor probe for sensing the NOx concentration and a Sensor Control Unit (SCU) for command and control purposes. These sensors communicate over Controller Area Network (CAN) interface.

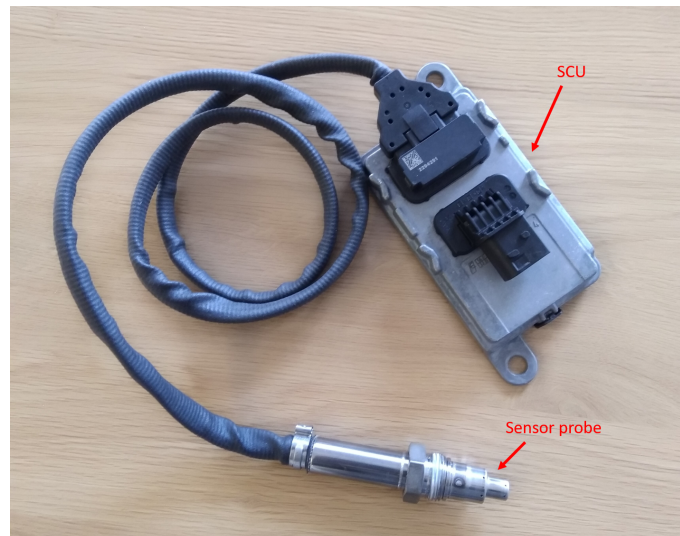


Figure 2.3: NOx sensor.

2.2.2 Wide band lambda sensor

Wide band lambda sensors, see Figure 2.4 also called oxygen sensors measure the oxygen concentration in exhaust gas. Based on the output of this sensor, the air-fuel ratio in internal combustion engine is optimized for better fuel consumption efficiency and reduced emissions. These sensors are made of zirconia based solid-state electro-chemical Nernst cells [16]. The functioning is similar to O_2 pump cell of NOx sensor explained in Section 2.2.1.



Figure 2.4: Wide band lambda sensor.

2.3 CAN interface

CAN [17] defined by ISO 11898 (International Organization for Standardization) standard, is a serial communication protocol where multiple nodes can transfer data on a single bus in a broadcast fashion. For physical layer, CAN uses differential signalling namely CAN-H (CAN High) and CAN-L (CAN Low) on twisted copper wires.

The two most common CAN standards are CAN-HS/FD (CAN High speed/ Flexible datarate) and CAN-LS/FT (CAN Low speed/ Fault tolerant) [18]. CAN-HS/FD (ISO 11898-2) has data transfer rate of 1 Mbits/s or higher and uses $120\ \Omega$ as bus terminal resistor whereas the later CAN-LS/FT (ISO 11898-3) can go up to 125 kbits/s and uses $100\ \Omega$. The sensors under test in this project are based on CAN-HS/FD.

CAN is a carrier-sense, multiple-access protocol with collision detection and arbitration on message priority (CSMA/CD+AMP). Hence, before sending the data on bus, each node waits for defined time. If two nodes try to send the data at the same time, a bit-wise arbitration method on the identifier field of CAN frame is used to decide the node priority. Based on identifier length, there are two types of CAN frames: standard CAN (11-bit identifier) and extended CAN (29-bit identifier). Extended frame format is used to communicate with sensors in this project. The extended CAN frame format as shown in Figure 2.5 [18].



Figure 2.5: Extended CAN frame format [18].

3

Method

The design and implementation plan for test-rig is explained in this chapter. Integral modules of both hardware and software are discussed along with details of test cases to be performed for further evaluation.

3.1 Test-rig hardware components

The test-rig consists of mainly a test cell to provide the required test environment, Compact Re-configurable IO modules (cRIO) as main controller, power supplies and laptop as shown in Figure 3.1.

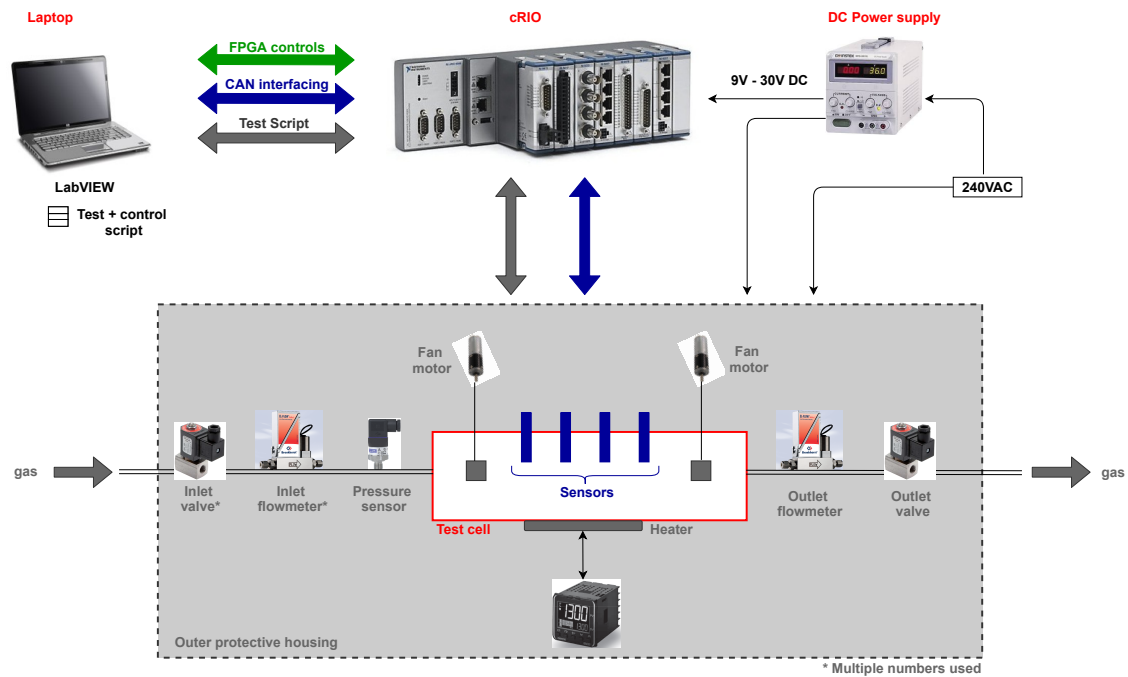


Figure 3.1: Block diagram for test-rig setup.

3.1.1 Test cell

To facilitate sensor testing, various equipment/ components are used. First, a thermally insulated and gas sealed metal box called "Test cell" of around 26 cm x 10 cm x 20 cm (LxWxH) is manufactured within Scania CV AB. The sensors under test are mounted on this test cell in such a way that the sensor probes are exposed to

3. Method

the gaseous environment inside. Following are the other component incorporated for testing:

- **Heater:** A 240 VAC cartridge heater of type HS/VDE (Harmonized System code/ Verband der Elektrotechnik) is used to vary the temperature inside the test cell during testing. The heater is controlled by relay signals from a temperature controller and a maximum temperature of 500 °C is allowed.
- **Temperature controller:** A 240 VAC digital temperature controller is used to change temperature of heater element. It is connected to cRIO's NI9871 C-series plug-in module [19] over RS485 interface for remote command and control. It continuously reads the test cell temperature from a mounted temperature sensor (Pt100) and generates relay output signal for heater based on the input commands from cRIO. The hardware pin connectivity to cRIO is shown in Figure 3.2.

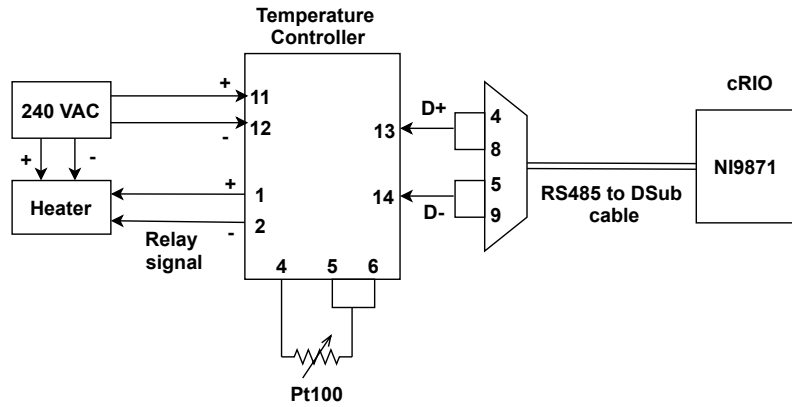


Figure 3.2: Hardware pin connections between temperature controller and cRIO.

- **Solenoid Valves:** Multiple 2/2 way solenoid valves are mounted on test cell for input and output gas flow. A total of five valves are used, four for input gas (air, nitrogen, NOx1 and NOx2) and one for output. These are remotely controlled by cRIO's NI9485 C-series plug-in module [20] for relay control. In addition, a safety valve for 1 bar pressure is also incorporated within the test cell. The hardware pin connectivity for one valve to cRIO is shown in Figure 3.3.

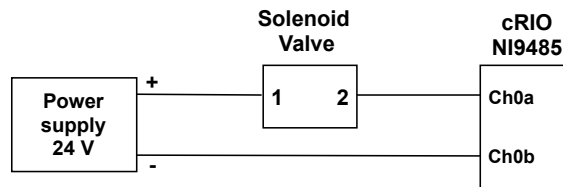


Figure 3.3: Hardware pin connections between solenoid valves and cRIO.

- **Temperature sensor:** Multiple Pt100 resistance temperature detectors are mounted on various locations inside test cell and directly by cRIO's NI9216

C-series plug-in module [21] through 4-wire temperature measurement.

- **Fan:** Fans with DC motor are also included for necessary gas circulation within the test cell. They are directly switched on by DC power supply.
- **Pressure sensor:** A pressure sensor of range 0-1.6 bar is mounted to read the gas pressure to the test cell. This sensor outputs current corresponding measured pressure which is converted to voltage by through a 2-wire sensing with $110\ \Omega$ precision resistor. The obtained voltage is read on cRIO analog input C-series plug-in module NI9220 [22]. The hardware pin connectivity to cRIO is shown in Figure 3.4.

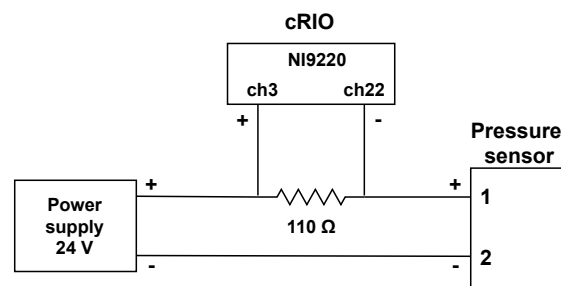


Figure 3.4: Hardware pin connections between pressure sensor and cRIO.

- **Flow controller with flow meter:** These accompany the input and output valves in the test cell for gas flow control and measurement. The flow control is done by analog voltage from cRIO's analog output C-series plug-in module NI9264 [23] whereas the measured flow (in V) is read by cRIO's analog input C-series plug-in module NI9220 [22] and converted to flow reading in Nominal Inch/minute (I_n/min). The hardware pin connectivity for one flow controller to cRIO is shown in Figure 3.5.

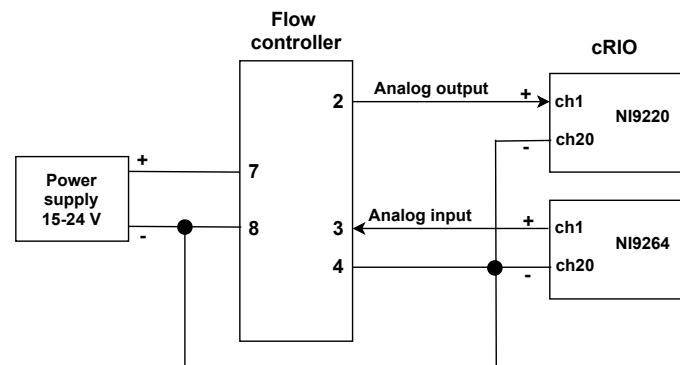


Figure 3.5: Hardware pin connections between flow controller and cRIO.

The entire test cell and related components are surrounded by a protective grid for safety reasons.

3.1.2 cRIO

The above mentioned test cell components require different Input/output (IO) interfaces like RS485, analog voltage, relay control etc for remote control. To communicate over these interfaces, cRIO-9057 [12] from NI is used. It is an industrial embedded controller with a modular architecture having a 1.33 GHz Dual-Core Intel Atom E3805 SoC (System on Chip). The main test logic and controlling of cRIO is done in LabVIEW, which is a graphical programming tool.

A total of eight C-series plug-in modules are used in this project. Table 3.1 summarizes their type, quantity and the test cell component controlled by each.

Table 3.1: cRIO plug-in modules.

Name	Interface	Quantity	Test cell component
NI9871	RS485	1	Temperature controller
NI9860	CAN	2	NOx Sensors
NI9216	4-wire temperature	1	Temperature sensors
NI9220	± 10 V analog input	1	Pressure sensor, Flow meters
NI9264	± 10 V analog output	1	Flow controllers
NI9485	Relay output	2	Solenoid Valves

3.2 Test-rig software components

The entire test-rig software logic is divided into three main parts: FPGA (Field Programmable Gate Array) configuration, CAN interfacing and test script as shown in Figure 3.1.

3.2.1 FPGA configuration

Most of the plug-in modules as mentioned in Table 3.1 communicates to the main cRIO SoC through individual on-board Xilinx Artix-7 7A100T FPGAs [24]. To configure these FPGAs, FPGA interfacing support and Real-time scan engine support are available in LabVIEW. The later is chosen for this project owing to its simplicity. Exception to this are NI9871 [19] (for RS485) and NI9860 [25] (for CAN) modules which are controlled by LabVIEW's ModBus communication protocol and NI-XNET interface respectively.

3.2.2 CAN interfacing

The NOx sensors communicate over CAN interface. A database container file (.dbc) is created based on the CAN protocol definition of NOx sensor by manufacturer. This .dbc file facilitates LabVIEW to input CAN command frames to sensor and read output frames. XNET Application Programming Interface (API) are used to read CAN frames in LabVIEW. The logic is further developed in the form of a state

machine to continuously log and save sensor data in a pre-defined file location. Figure 3.6 shows the software logic flow for CAN interfacing. DPE and Self diagnostics concepts are explained in detail in Section 3.4.

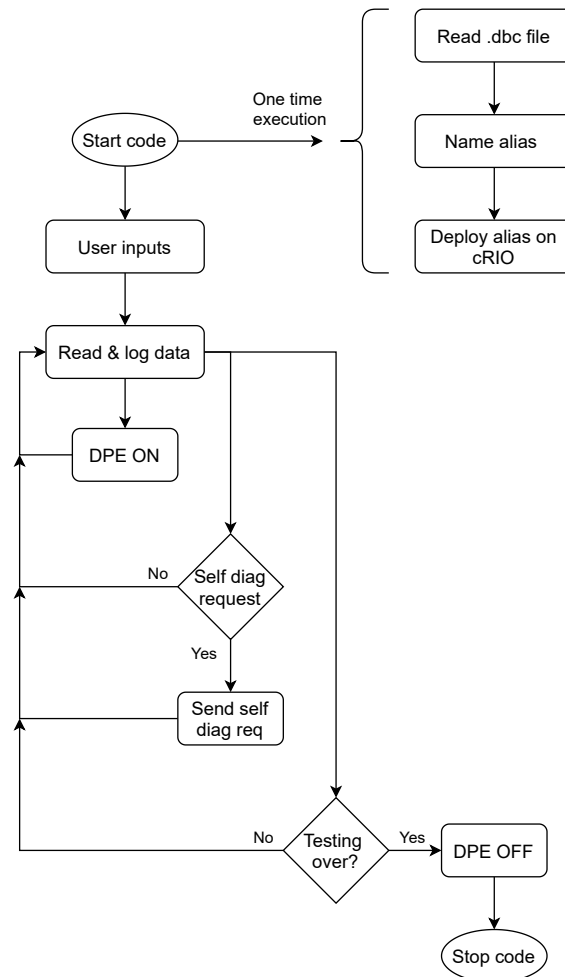


Figure 3.6: Flowchart for CAN interfacing logic.

3.2.3 Test script

The test cell equipment setting is done through a script format where in all the required test parameters are set and uploaded. To read and execute this input script, a background code is used which is customized version of inhouse developed STP (Scania Test Platform) [26] control scripts. The purpose of having a test script language is to add flexibility for the user without increasing Graphical User Interface (GUI) complexity. Figure 3.7 shows an example script for controlling two temperatures and a valve.

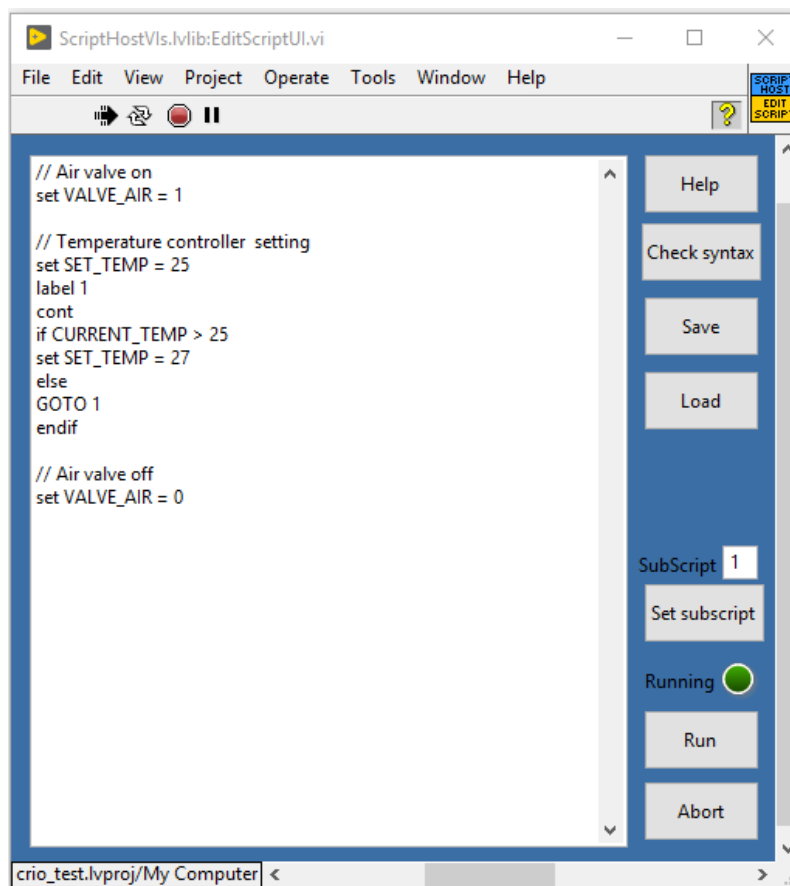


Figure 3.7: Example test script.

3.3 Test-rig software flow plan

The overall automated test-rig software logic is divided into four phases: Initialization, Test configuration, Testing and Shutdown as shown in Figure 3.8.

- **Initialization phase:** In this phase, it is assured that communication is established between cRIO and all other test-rig equipment, and then sensors are power up by DPE ON signal.
- **Test configuration phase:** As per user requirement, input test settings are

uploaded. Based on that, commands are sent to required test cell components (valves, temperature controller etc). Continuous monitoring of equipment health status is done till the test environment inside test cell is stabilized.

- **Testing phase:** This is the main phase where actual testing is performed. Multiple parallel software routines run here for smooth execution of any test case. Also, sensor data logging and saving is carried out here in real-time.
- **Shutdown:** After successful completion of input test case, a series of commands are sent to bring the test cell at default state, which is followed by sensor power off. Either a separate script is loaded to carry out this phase or the closing sequencing can be added in the test configuration script after necessary wait commands.

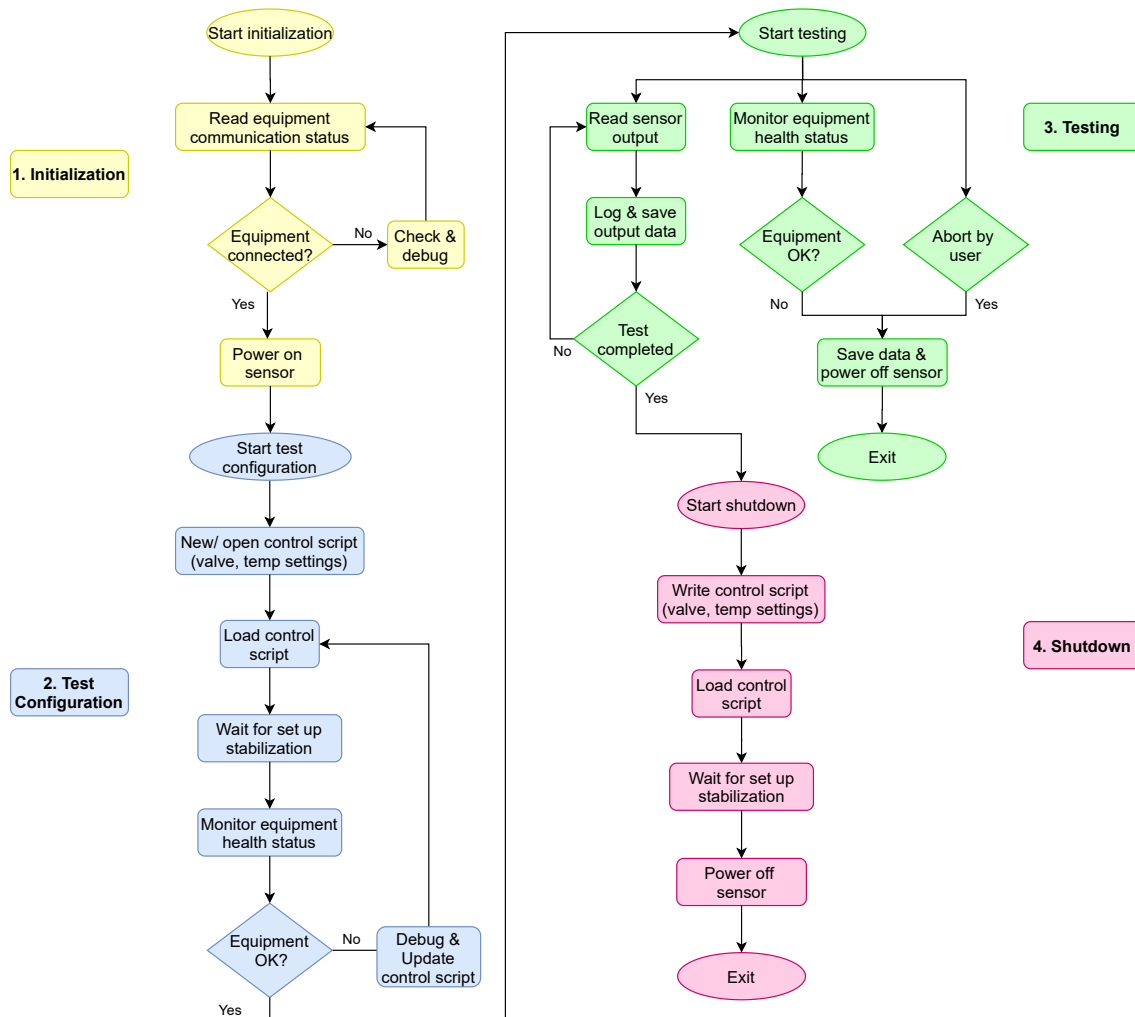


Figure 3.8: Overall software flow plan for test-rig.

3.4 Graphical User Interface (GUI) and Code explanation

LabVIEW is used as the main programming tool for entire software code in this project. A Virtual Instrument (VI) is the basic entity in LabVIEW for coding. It consists of front panel for user interaction and block diagram for background code and functionality. The control of each individual test-rig component is done through respective VI. Finally, all the VIs are called in a pre-defined manner from a main VI to carry out the test flow.

In this project, there are two main sets of VIs depending on the platform on which they run: computer and cRIO. The VIs which run on computer are auto-started by "launcher.vi". The VIs on cRIO are automatically started by executable "boot.vi" at the time cRIO is powered on and keeps running till cRIO is switched off. The interaction between computer and cRIO VIs are done through "Shared Variables".

Figure 3.9 shows the main GUI where user inputs are fed and equipment monitoring is done. The details and sequence of user inputs in above GUI are as below:

1. This is the directory path where sensor output data files are saved.
2. The cRIO has two modules for CAN interfacing, each having two CAN port. Hence, a total of four CAN ports/ buses are available. Each CAN port can communicate with multiple sensors with different IDs. In this code, four types of NOx sensors are planned to be tested: two input sensors, ATI1 and ATI2, and two output sensors, ATO1 and ATO2. Once the sensors over respective CANs are selected, "Enter" is pressed.
3. After power on, the internal heater in NOx sensors heats up to 200°C and wait for Dew Point Enable (DPE) on signal from engine. The signal signifies that no water is present in vehicle tail-pipe and it is safe to start sensor as NOx sensor are prone to failure in presence of water. For testing independent NOx sensors in this project, user sends a DPE on/ off signal to switch on/ off the sensors.
4. The NOx sensors have a self-diagnostic feature which can be turned-on/ off based on user requirements. This is optional.
5. Apart from main sensor data, there are auxiliary sensor data (like heater information, correction factors, address claiming etc) sent by sensor on power on. This data can again be requested on user demand. This is optional.
6. Option is available to user to either test with manual controls or automatic with control scripts. In case of manual control, user needs to manually switch on/off valves with available push buttons and enter required temperature and gas flow values. In case of automatic control, user needs to upload pre-saved

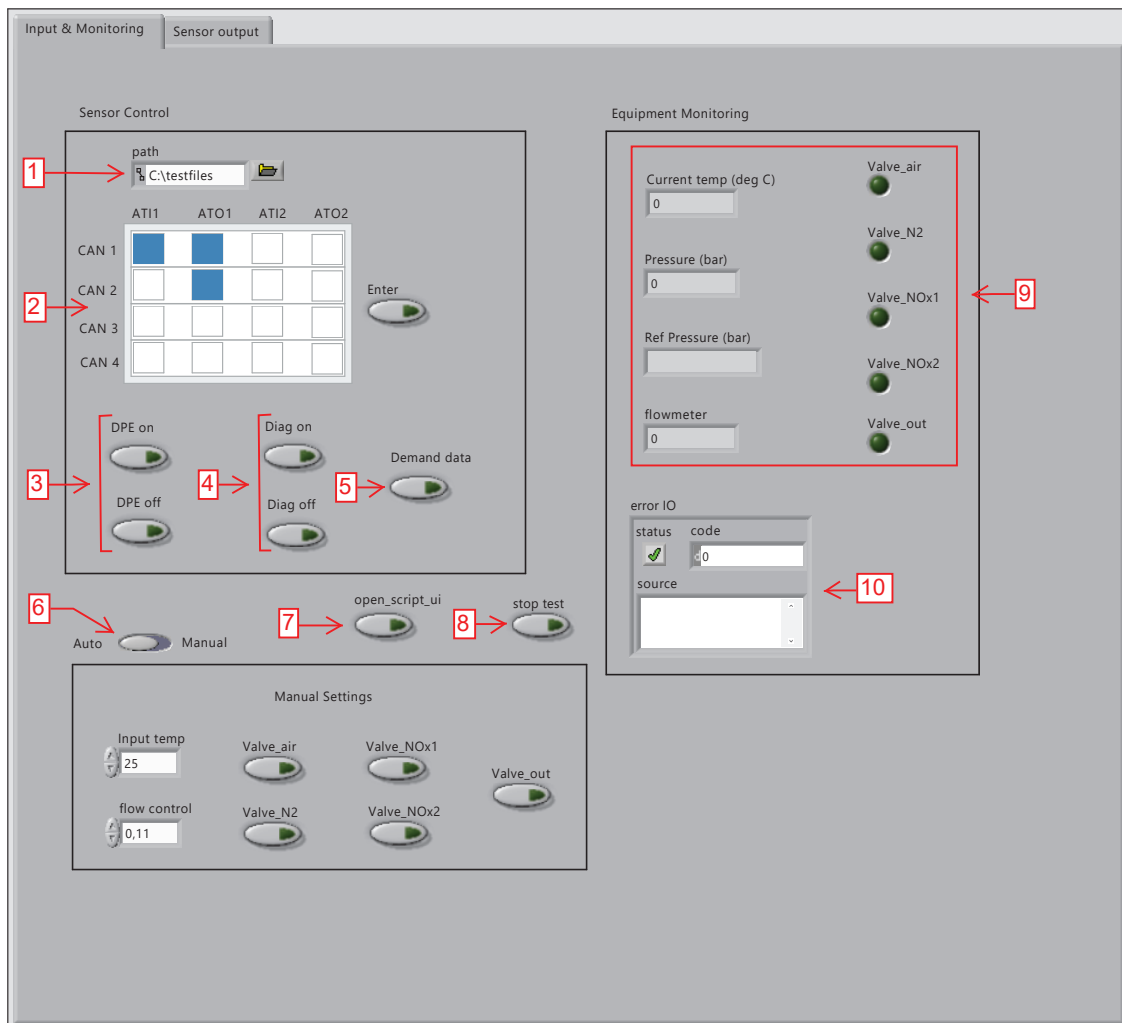


Figure 3.9: User input and monitoring GUI

control script file.

7. The control script is loaded with a separate VI which is part of Scania Test Platform (STP) routines. This is required to set parameters for controlling test-rig components: temperature controller, solenoid valves etc. Figure 3.7 shows control script window.
8. Once testing is done, "Stop Test" is pressed to close all the subVIs. Abort can be pressed for emergency situation.
9. The test cell equipment real-time data like test cell temperature, relative pressure and gas flow can be monitored directly from GUI. Real-time atmospheric reference pressure is directly available from Scania's other test set-ups and linked to this test-rig software code. The valve indicators show the position of each valve.

3. Method

- Errors in code are propagated and displayed to user for trouble-shooting purpose.

Figure 3.10 shows the output GUI where main sensor output signals: NO_x and O₂ concentration, status of NO_x, O₂ and self-diagnostic signals are displayed. Also, the data 2 parameters which may be required before starting the test are displayed for user information. The remaining sensor data is stored in a .txt file in the path entered by user for further analysis.

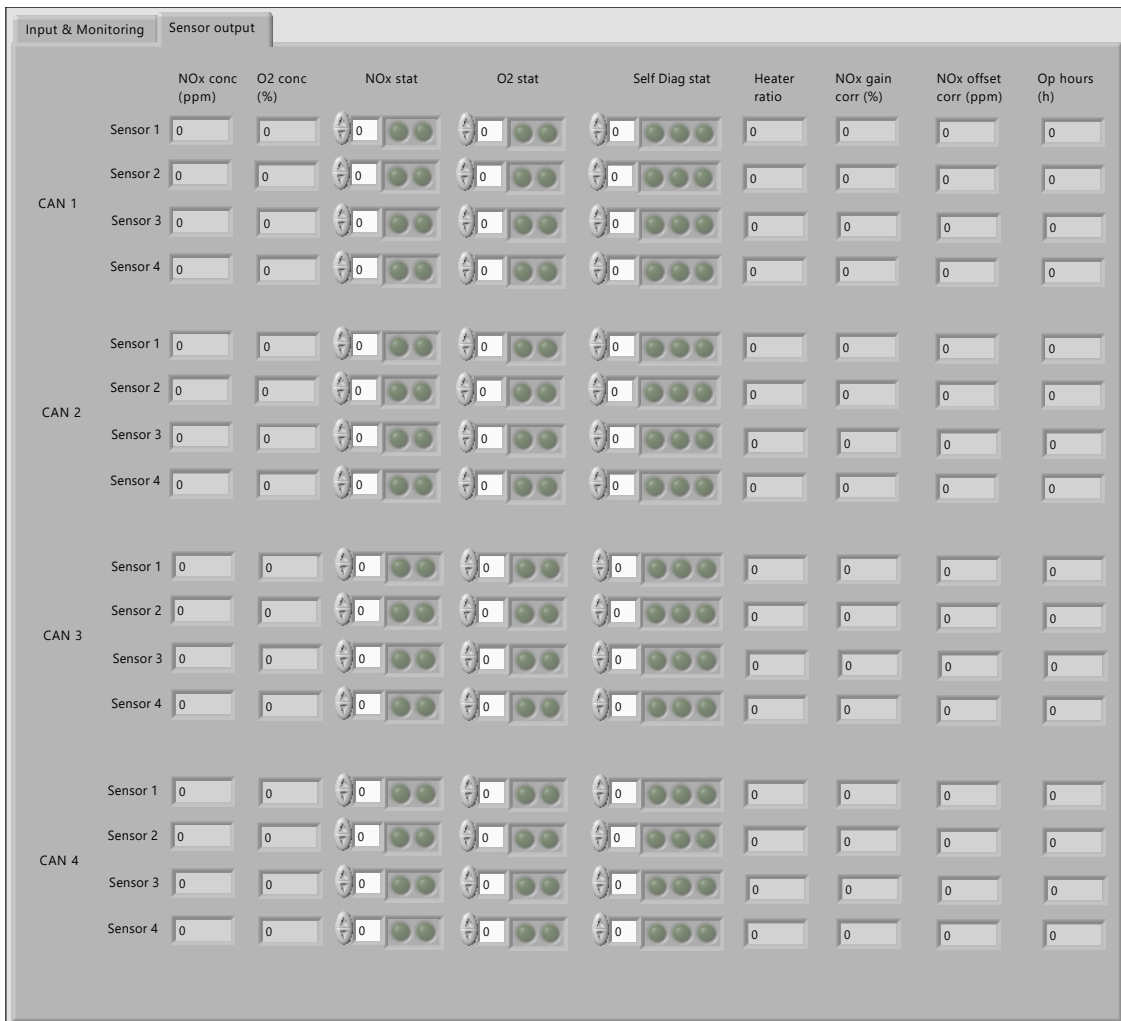


Figure 3.10: Output GUI

3.5 Experiment plan

Once the test-rig is set up, the following two types of test cases are planned to evaluate the performance of this automatic test-rig:

- **Gas variation:** As mentioned before, sensors are tested in three different gas environments: air, nitrogen and NO_x of known concentration. Sensor response is observed by switching between these gases and repeatability performance of test-rig is also tested. A control script to open and close required gas valves in a pre-defined sequence is written for this test execution.
- **Temperature variation:** In this test case, the sensors are tested for varying temperature for a given gas concentration. The temperature variation is done either in a ramp form or in steps between two values. Control scripts are written for both the formats.

4

Results and Discussion

The test cases performed with the developed automated test software are explained in this chapter along with the results and deliberations during comparison with manual test-rig.

4.1 Testing Scenario

The NO_x sensor testing was conducted in three gas environment: air, nitrogen and NO_x. Air and nitrogen were fed through the available wall-mounted gas pipes while NO_x was fed through a gas bottle with a NO_x concentration of 489 ppm.

Due to the delay in delivery of new gas-sealed test cell from Scania CV AB workshop, the testing was carried out in the old test cell which can take maximum four NO_x sensors as shown in Fig. 4.1. Most of the components planned for new test-rig in this project were connected to the old test cell for testing. Since this old test cell was pre-installed with an output valve for continuous gas outlet and not suitable to perform temperature variation test, temperature controller, heater, and output solenoid valve were not connected.

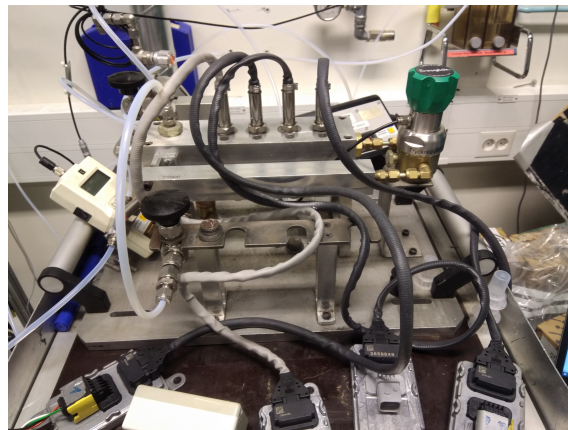


Figure 4.1: NO_x sensors mounted on old test cell.

Fig. 4.2 shows the overall test-rig set up and following is the list of components used in the final testing:

- cRIO with all modules mentioned in Table 3.1
- NOx sensors : ATI1 (Qty 1), ATO1 (Qty 2)
- Solenoid Valves (Qty 4) : One each for air, nitrogen and NOx with two different concentrations.
- Pressure sensor (Qty 1)
- Flow controller (Qty 1)
- Power supply
- Laptop

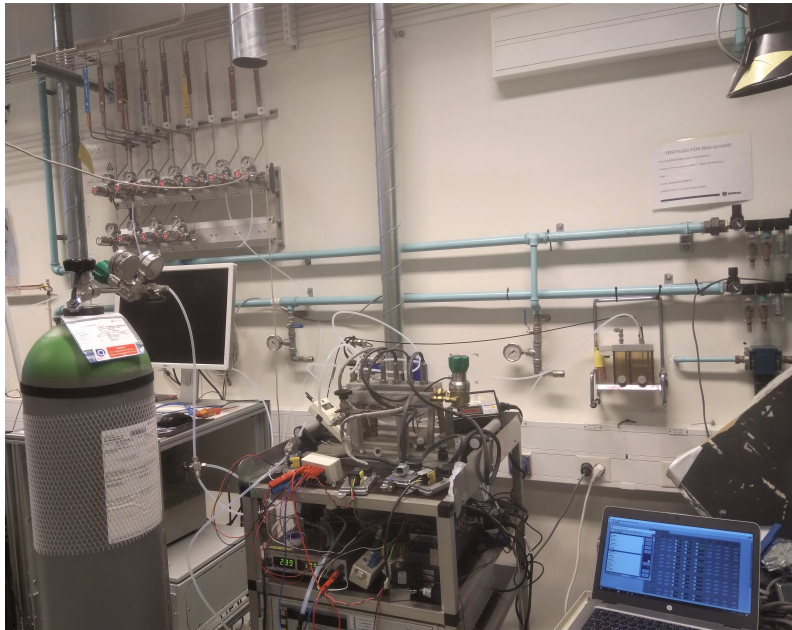


Figure 4.2: Final test set up.

4.2 Test cases

The main test case carried out in the test-rig was a combination of all three gas inputs (air, nitrogen and NOx) in both manual and automated manner. Three sensors were tested together: One ATI1 and one ATO1 were connected on CAN1 and another ATO1 was connected on CAN2. Hence the test case covers the two interface possibilities: different sensors on same CAN and same sensors on different CANs.

4.2.1 Test case 1

The first test case carried out was a manual one where the test-rig components (valves, flow controller etc) were controlled manually by user. Following are the detailed input settings for this test case:

Total test time = around 40 min

NOx input concentration = 489 ppm

Flow control = $0.11 \text{ l}_n/\text{min}$

Input gas valve opening sequence with 1 min wait in between each gas = 1 cycle

Air (5 min) > NOx (10 min) > Air (10 min) > N2 (5 min) > Air (5 min)

As explained in Section 2.2.1, the NOx sensors measure both the NOx and O_2 levels and send these values over CAN. The NOx measurement test results for three sensors for above mentioned test case is shown in Fig.4.3.

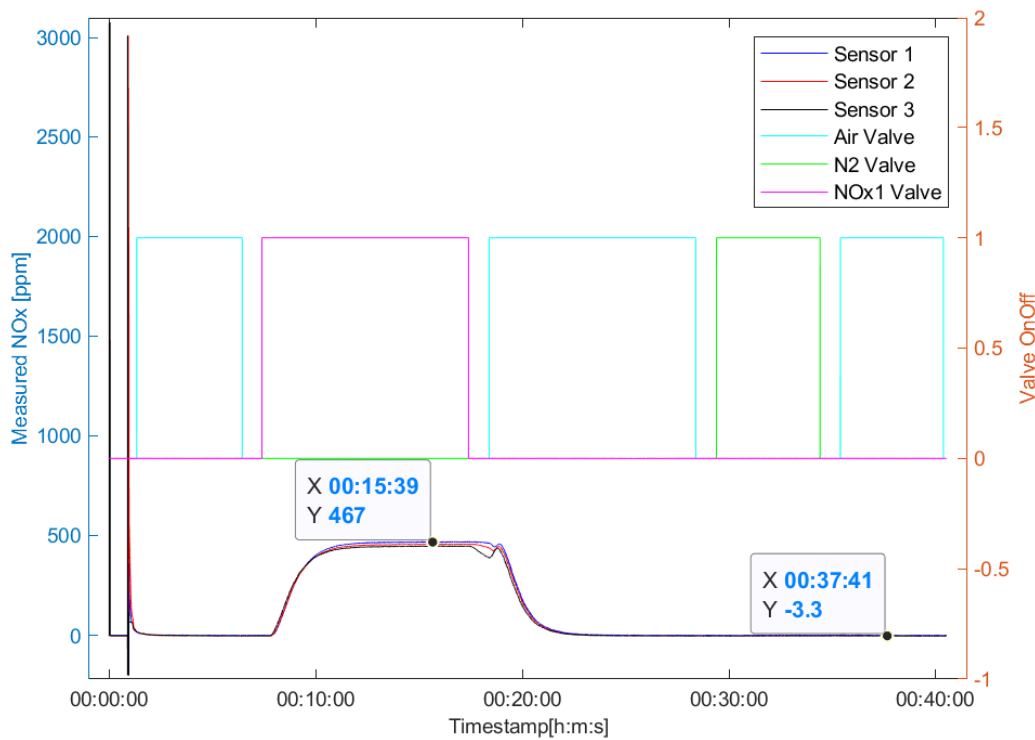


Figure 4.3: NOx measurement for Manual test case. Left y-axis shows NOx values in ppm and right y-axis shows valve position (0=off, 1=on). The sensors NOx measurement increases when NOx valve is on and decreases to 0 for other gases.

As seen in above figure, when the input valve for NOx was switched on, there was an increase in measured NOx values from all three sensors. The input NOx concentration was 489 ppm whereas the measured NOx concentration for all three sensors was ≈ 467 ppm. As per sensor datasheet, the sensitivity of these sensors is $\pm 10\%$ for 100-500 ppm. Also, before entering the test cell, the input NOx gas was first humidified in a water bubbler which further reduces the gas concentration by $\approx 2\%$. Hence, a measured output of 467 ppm is within the expected output range.

In presence of air or nitrogen gas, the sensor NOx output decreases to zero as expected. It is also noticed that the rise time for sensor response is slightly larger than

4. Results and Discussion

the fall time which can be attributed to difference in gas pressure for supplied gases and performance of gas regulator for different input pressures.

After the sensors receive Dew Point Enable (DPE) signal from user, the internal sensor temperature is raised to 800 °C by in-built heater. Once this temperature is stabilized the NOx and O₂ status signals become valid. The initial spikes in the NOx measurement were the dummy values sent by the sensors before the NOx status became valid. The O₂ measurement test results for three sensors for above mentioned test case is shown in Fig.4.4.

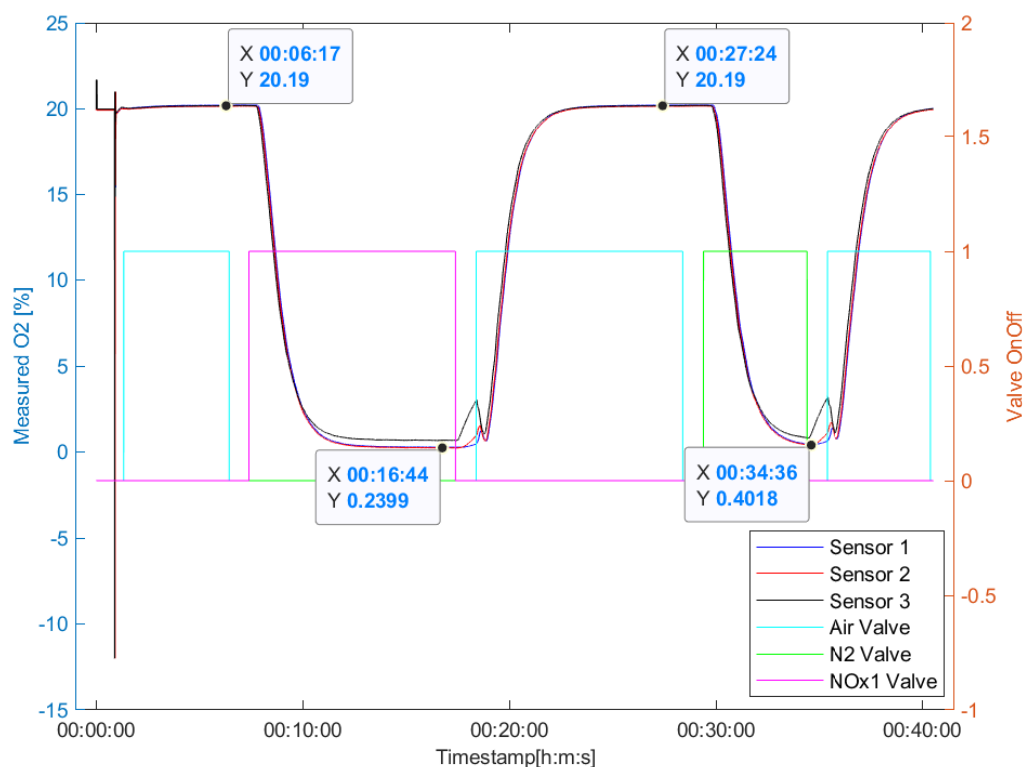


Figure 4.4: O₂ measurement for Manual test case. Left y-axis shows O₂ values in % and right y-axis shows valve position (0=off, 1=on). The sensors O₂ measurement increases when air valve is on and decreases to 0 for other gases (nitrogen and NOx).

As seen in these figures, when the input valve for air was switched on, there was an increase in measured O₂ values from all three sensors. The measured O₂ is ≈ 20% which is normally the oxygen concentration in air. It is also seen that the O₂ values decrease in presence of other gases, NOx and nitrogen in this case. Fluctuations in sensor response are observed whenever there is change in gas environment to air. One of the reasons may be due to the sudden change of pressure during valve maneuvers but this can be further analyzed.

Since, during the second fall instance (5 min nitrogen environment) the sensor output

could not reach minimum value; hence it can be concluded that a longer time is required to get stabilized output. Similar to NO_x results, the initial spikes are the dummy values before the O₂ status signal became valid and the response rise time is larger than fall time.

4.2.2 Test case 2

The next test case carried out was a fully automated test case where all the test-rig components were controlled through a control script. Because of ease of test conduction in automated case, two test cycles were planned. All the input settings for first cycle were kept similar to the manual one in Section 4.2.1. The second cycle contained slightly longer time to cross-check the stabilization time for sensor output.

Total test time = around 90 min

Input gas valve opening sequence with 1 min wait in between each gas = 2 cycles
 Air (5 min) > NO_x (10 min) > Air (10 min) > N₂ (5 min) > Air (5 min) >
 Air (5 min) > NO_x (15 min) > Air (10 min) > N₂ (10 min) > Air (5 min)

The NO_x measurement test results for three sensors for above mentioned test case are shown in Fig.4.5.

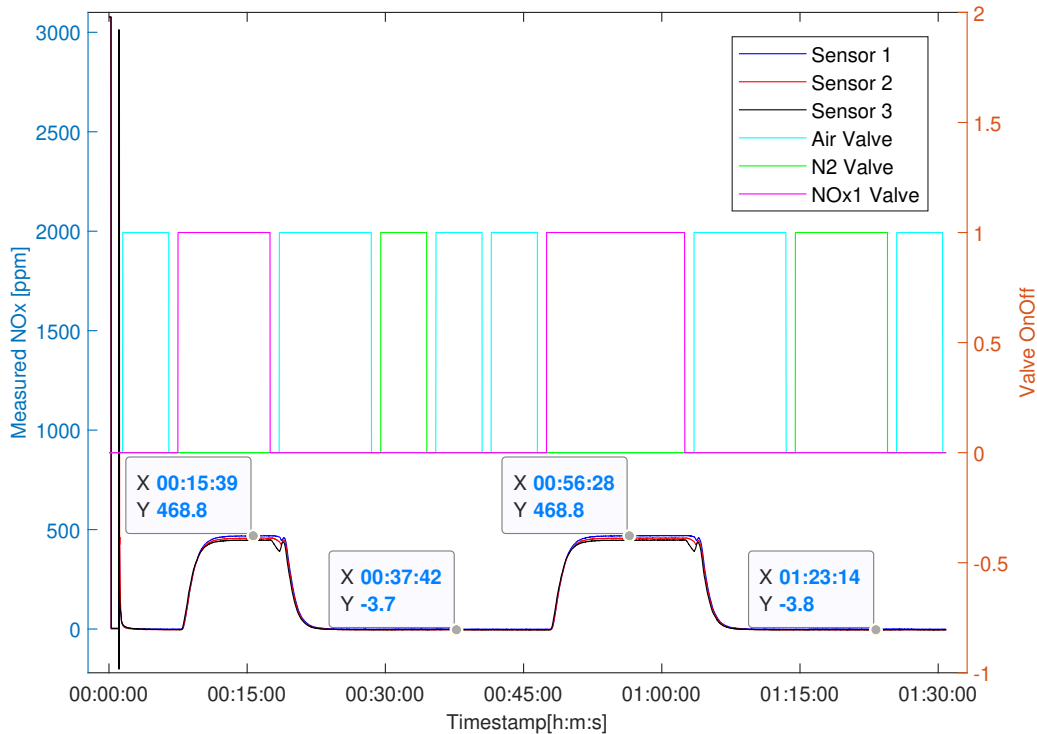


Figure 4.5: NO_x measurement for Automatic test case. Left y-axis shows NO_x values in ppm and right y-axis shows valve position (0=off, 1=on). The sensors NO_x measurement increases when NO_x valve is on and decreases to 0 for other gases.

4. Results and Discussion

Similar to the manual test results, increase in NO_x measurement is seen when NO_x valve is switched on. Since, for all three sensors the measured NO_x concentration for both first cycle (10 min) and second cycle (15 min) is same, hence it can be concluded that for a gas flow of 0.11 l_n/min, 10 min is sufficient to get stabilized NO_x values.

On comparing the results to the manual one in Fig.4.3, the NO_x values at given time instant are approximately same. For example at timestamp of 00:15:39 the NO_x concentration measured in manual case is 467 ppm where as for automated case it is 468.8 ppm. The small difference may be attributed to absence of intermittent delays in valve maneuvers during automated case resulting in early stabilization of sensor outputs; assuming that the NO_x concentration variation between switch on/off/on cycles is better than ± 1 ppm. Fig.4.6 shows the zoomed in plot for first cycle of NO_x gas.

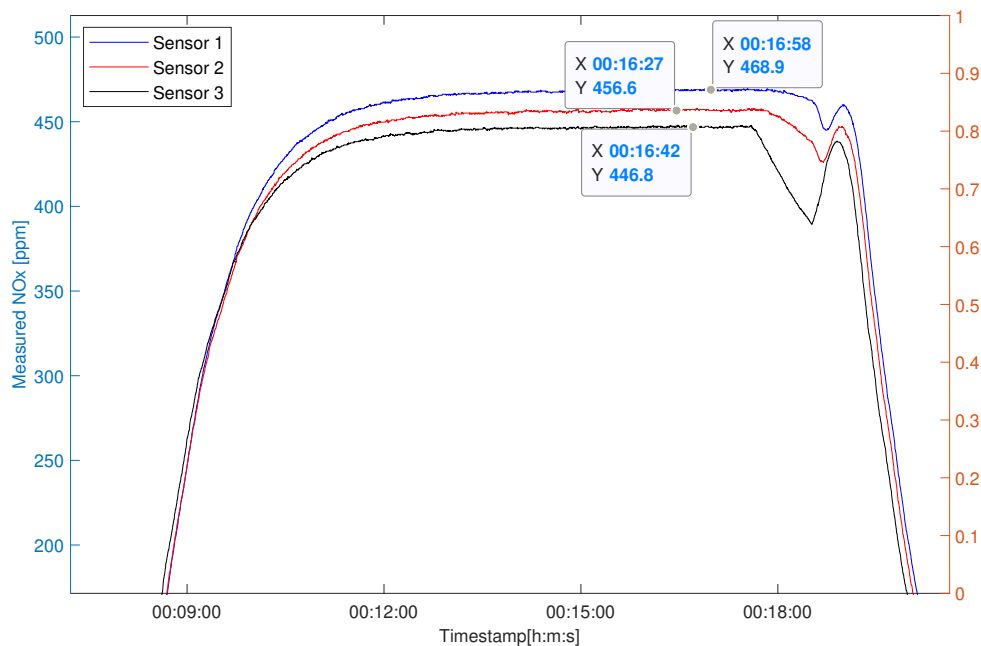


Figure 4.6: Zoomed in NO_x measurement for Automatic test case. Sensor 3 has faster response while sensor 1 measurement is more accurate.

It is observed that the response of sensor 3 is faster than other sensors but has higher fluctuation. Also, its measurement is $\approx 7\%$ off, however it is still within specification. Sensor 1 measured output is closest to expected output range. The O_2 measurement test results for three sensors for above mentioned test case are shown in Fig.4.7. As seen in these figures, the measured O_2 values follows the expected pattern with respect to the input air valve. It is also noticed that with this gas flow, 10 minutes time is sufficient to get a stable 20% O_2 levels.

Finally, it can be concluded that all three sensors seem to behave in similar fashion

for both NO_x and O₂ measurements. However, sensor 3 shows some deviations and fluctuations compared to others.

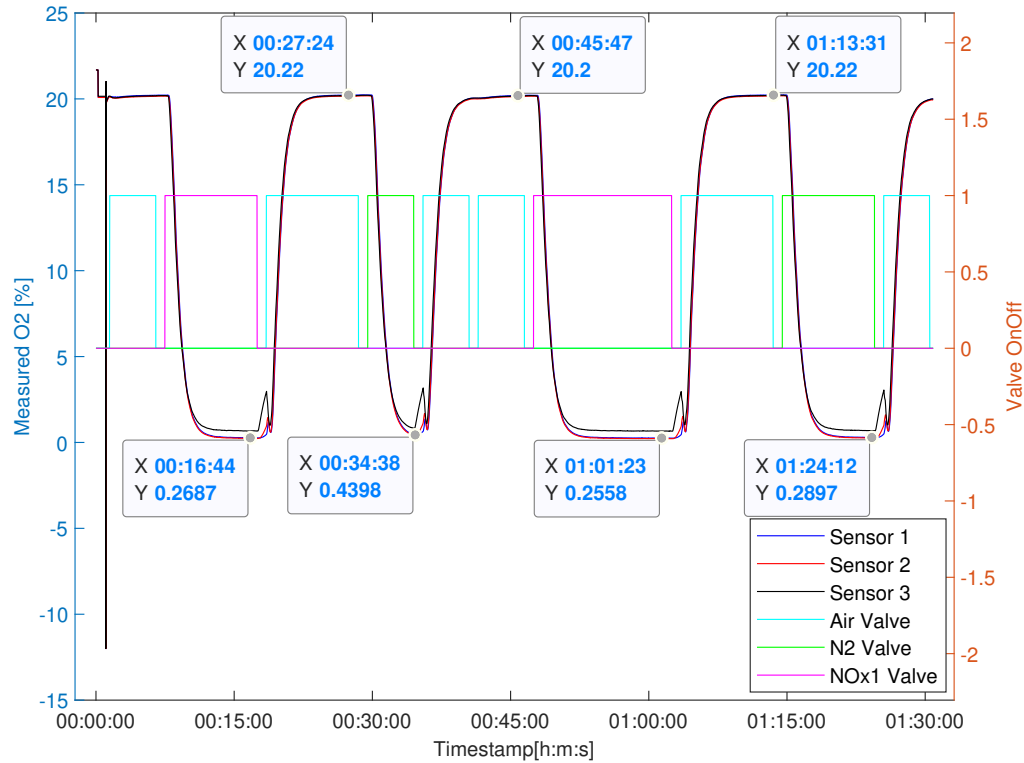


Figure 4.7: O₂ measurement for Automatic test case. Left y-axis shows O₂ values in % and right y-axis shows valve position (0=off, 1=on). The sensors O₂ measurement increases when air valve is on and decreases to 0 for other gases (nitrogen and NO_x).

4.3 Automated test-rig comparison

To evaluate if the designed automated test-rig is a suitable substitute to available manual test-rig, two parameters were checked. First, the operator/ operating time to perform a given number of tests for automated test-rig was compared to that of manual test-rig. Next, to check the repeatability, the input valve switching performance were compared for automated and manual tests. Since the temperature variation could not be performed, the repeatability performance during temperature cycling was not included during comparison.

4.3.1 Operator/ Operating time

Multiple test cases were conducted to observe the operator/ operating time. Depending upon the test cases, during the manual test a continuous presence of operator is required specially for valve control. However, this is not the case for automatic test as all the test component input and controls are pre-defined in a control script. Once, the script is loaded by operator, the testing continues in a complete automatic fashion with no further requirement of operator.

For example, for test case 1 in Section 4.2.1 which ran for 40 min, the active operator time was almost 20 min throughout the test. There were total six times of valve maneuvers apart from the initial time for program setup and running. This active operator time varies with the how frequently the valves need to be changed.

Opposite to manual case, for test case 2 in Section 4.2.2 the active operator time is significantly reduced and only limited to the time required for running the program and uploading the script. One of the major advantage with automatic testing was that a much longer test case with multiple cycles can be run without overloading the operator. As seen in this test case out of the total run time of 90 min, the active operator time was ≤ 1.5 min.

In addition, the operator time will be greatly influenced during temperature variation test cases as it will require a constant user input to temperature controller. Where as for automatic testing, similar to valve controls, the temperature controller can be directly controlled through control script and needs no operator intervention. To get a detailed analysis of active operator time, several test cases were carried out. It is seen that automatic test-rig saves $\approx 50\%$ of operator/ operating time compared to manual one.

Hence, this test-rig saves operator time in proportion to time to perform test. Usage of predefined test scripts effectively means that operator time is reduced to sensor installation/ replacement time. Of course, there will be some downtime required for writing these test script which may or may not be equivalent to designing the test for manual case depending on user competence. However, in this project only the test operating time is considered for comparison of both the manual and automated case.

4.3.2 Repeatability

A test case is carried out where the input valves were switched on and off in both manual and automatic manner. In manual case, depending upon the test case requirements the user controls the test-rig components through manual settings in GUI. In automatic test case, a pre-defined control script is uploaded which in turn controls all the test-rig components. Following is the input sequence for valve control:

```
Input gas valve opening sequence = 6 cycles
Air (5 s) > NOx (5 s) > Air (5 s) > N2 (5 s) >
Air (5 s) > NOx (5 s) > Air (5 s) > N2 (5 s) >
Air (5 s) > NOx (5 s) > Air (5 s) > N2 (5 s) >
Air (10 s) > NOx (10 s) > Air (10 s) > N2 (10 s) >
Air (10 s) > NOx (10 s) > Air (10 s) > N2 (10 s) >
Air (10 s) > NOx (10 s) > Air (10 s) > N2 (10 s) >
Air (2 min)
```

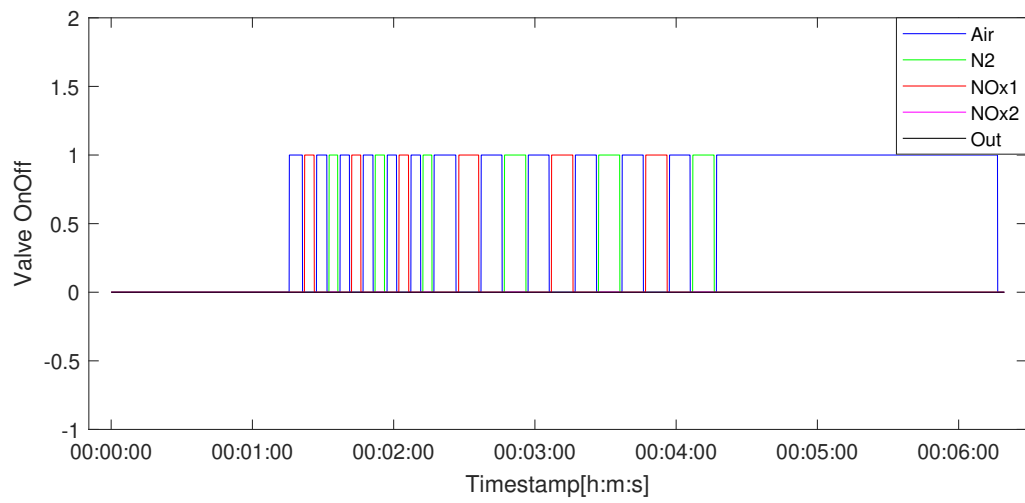
Total test time = around 6 min

Figure 4.8 shows the test results for above mentioned test case. As seen in this figure, during manual control, user has to first switch off the valve to first gas before opening next which results in some intermittent delays. Also, the initial delay in starting of test case may vary depending upon what other components (like flow controller) are to be controlled manually. For automatic control, all component inputs including valves are directly controlled by control script which can be run with a precision of milliseconds which further reduces the delay in test execution.

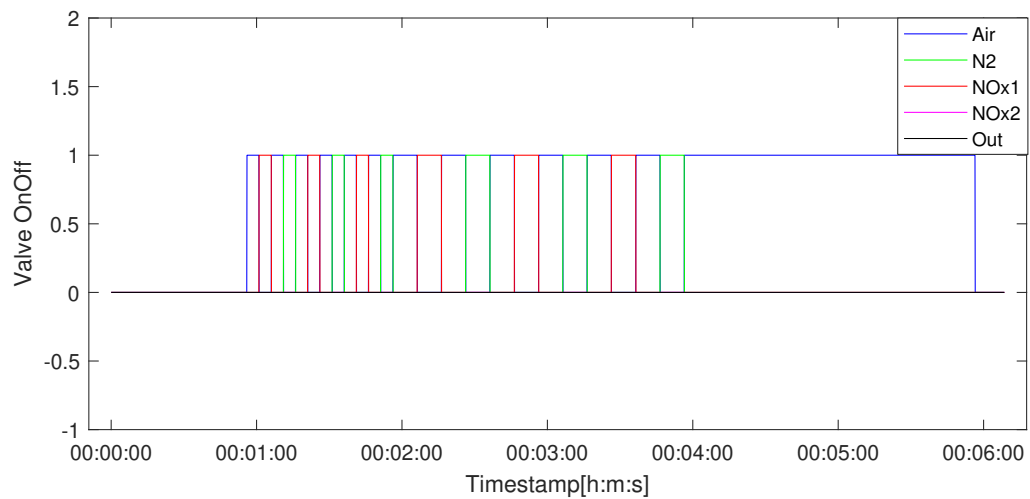
The difference in these intermittent delays for manual and automatic test are further analysed and shown in Figure 4.9. It is noticed that for a 6 min test, approximately 3 s delay is accumulated in manual test which amounts to 0.83%. Since, the delay is significantly less, hence it can be inferred that performance wise both manual and automatic test-rigs are same. However, this result may vary for other tests with different valve repeatability conditions. Although, no degradation in repeatability of measured values has been observed, but a more thorough evaluation should be carried out.

Repeatability tests can also be used for testing sensors with temperature cycling, however such tests could not be conducted due to limitations of resources as discussed earlier in this chapter.

4. Results and Discussion



(a) Manual



(b) Automatic

Figure 4.8: Valve repeatability test case. Manual testing has more intermittent delays during valves maneuvering compared to automatic one.

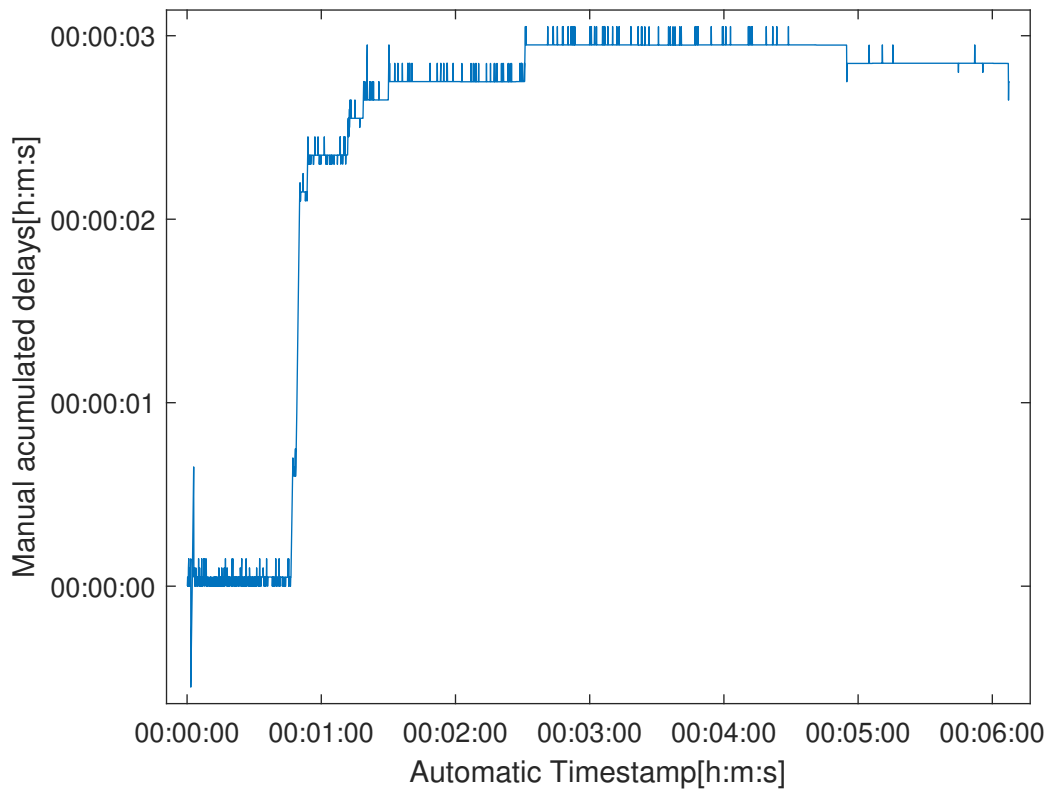


Figure 4.9: Accumulated delays in manual testing for test case in Section 4.3.2. Around 3s of delay is accumulated in manual test over automated for a total test time of 6 min.

4.4 Other sensor testing

It was also proposed to extend the project for testing other sensors like lambda and ammonia. The testing of lambda and ammonia sensors could not be carried out owing to other challenges. The lambda sensors available in Scania CV AB interfaced through analog signals instead of CAN. A custom-built cRIO plug-in powertrain module NI9757 [27] was attempted to directly communicate with these sensors, but had some interfacing issues. Ammonia sensors were dropped during initial planning phase due to unavailability of ammonia gas for testing.

5

Conclusion

This project was started with the aim to completely automate the NOx sensor test-rig which is currently a semi-automatic one in Scania CV AB. Apart from sensors, multiple test components (solenoid valves, flow controller, temperature controller, heater etc) were planned for this automatic test-rig. In addition, a gas-sealed test cell was planned to mount around eight sensors. cRIO and LabVIEW were the main hardware and software chosen in this project.

The project was equally balanced between various hardware and software fields encompassing interfacing, connectivity and communication of test-rig component, logic and code implementation in a modular way for multi-sensor multi-CAN scenarios. The three main parts of software development were: FPGA configuration for cRIO modules, CAN interfacing for sensors, and control script for command and control of test-rig components. cRIO FPGAs were configured using LabVIEW's Scan engine mode. For sensor communication over CAN, XNET APIs were utilized. All the sensor data were continuously logged and saved in real time for further analysis.

Due to the delay in delivery of new test cell, the final testing was carried out on the old test cell with all other components from new test-rig. Several test cases were run in three gas environment (air, nitrogen and NOx) and the measured NOx and O_2 data were plotted to check the sensor response. It was observed that the sensor behaved withing expectation with variation in gas inputs. For a 489 ppm NOx input concentration, the sensor detected in the range 446 ppm-468 ppm and for normal air environment, the detected O_2 level was 20%. It is also noted that the stabilization time for sensor outputs varies with the flow of gas inside the test cell. For a NOx flow rate of around 0.11 l_n/min, the sensor reading takes around 10 min to be stable.

Finally, the automatic test-rig was compared to manual one with respect to operator/ operating time and repeatability performance. It was seen that automatic test-rig saves around 50% of active operator time and allows the tests to be conducted for much longer time and for multiple cycles without overloading the operator. Regarding repeatability, it was noticed that the automatic test can be run more smoothly without any delays over manual one. The repeatablilty performance was checked only for gas variation and could not be tested for temperature variation due to incompatibility with old test cell. Hence, it was concluded that the automatic test-rig can be a suitable substitute for the manual one especially when there is a need for testing huge numbers of faulty NOx sensors from field.

6

Future Works

As with every project, there is always scope of further improvement which is discussed in this chapter. These are the suggested improvements for the developed automated test-rig (hardware and software) or further scope of work that can be done using this test-rig. Some of the action points which were earlier planned as part of this project but could not be carried out due to various constraints are also included here.

- NOx sensor sends several data packets over CAN. Currently, only single packet data are read and recorded in this project. The LabVIEW code for CAN communication is implemented using XNET APIs which has limitation for multi-packet data. Although, the current data fulfil the project requirement for testing NOx sensors, it will be beneficial to also record remaining multi-packet data.
- As mentioned in Section 4.1, due to resource limitation effects of temperature variation on sensors can not be evaluated which was earlier planned as part of project. The software code for temperature variation is implemented and bench testing with temperature controller (24 V) is carried out. However, once the planned test cell is received from workshop, actual testing needs to be performed with 240 VAC temperature controller and heater.
- The test-rig can be further modified for faster gas source switching. To achieve this, small valve controlled gas volumes that are filled with 1 bar gas pressure needs to be installed. This also facilitates actual testing of sensor response time.
- Currently, the communication status of all test equipment is monitored as user is intimated on main GUI in case of error. However, there is further scope to extend the safety precautions while testing with various gas environment (especially NOx which is poisonous in nature) in terms of emergency procedures, safety analysis and CE (Conformité Européenne) marking.
- Initially, automated testing of other electro-chemical sensors, lambda and ammonia, were planned in this project. However, ammonia sensors were dropped in planning phase due to unavailability of ammonia gas at Scania CV AB. The available lambda sensors do not communicate over CAN as with NOx sensors. Efforts have been put to use a customized powertrain cRIO plug-in module

(NI9757) for communicating with lambda sensors. This calls for cRIO to be used in hybrid mode as other plug-in modules are currently in Scan engine mode. For hybrid mode an empty slot is required between Scan engine and powertrain module which is unavailable. Owing to these issues, lambda sensor communication and testing could not be attempted further in this project. This can be rectified first by planning an extended cRIO chassis with required empty slots and further troubleshooting hybrid mode issues.

- Based on interaction with Scania CV AB personnel and research during literature survey, it was found that the NOx sensors from field exhibits various faulty outputs: oscillation in measured data, stuck at particular value, wrong measured output etc. Multiple tests need to be conducted with this developed automated test-rig to analyze these anomalies.
- Another important scope of this automated test-rig can be to compare the sensor performance from different manufacturers/ suppliers.

Bibliography

- [1] EU, “Commission Regulation (EU) No 582/2011,” *Official Journal of the European Union*, pp. 1–168, 2011.
- [2] J. E. Jonson *et al.*, “Impact of excess NO_x emissions from diesel cars on air quality, public health and eutrophication in Europe,” *Environmental Research Letters*, vol. 12, no. 9, Sep 2017.
- [3] R. B. Gurung *et al.*, “Predicting NO_x sensor failure in heavy duty trucks using histogram-based random forests,” *International Journal of Prognostics and Health Management*, no. ISSN2153-2648, 2017 008, 2017.
- [4] R. R. Yager *et al.*, “A soft computing approach to controlling emissions under imperfect sensors,” *IEEE Transactions on Systems, Man, and Cybernetics: Systems*, vol. 44, no. 6, pp. 687–691, 2014.
- [5] Y. y. Wang *et al.*, “NO_x Sensor Reading Correction in Diesel Engine Selective Catalytic Reduction,” *IEEE/ASME Transactions on Mechatronics*, vol. 21, No.1, 2016.
- [6] K. Kim *et al.*, “Ammonia cross-sensitivity elimination method of NO_x sensor for urea-SCR (Selective Catalytic Reduction) System,” *IEEE, 20th International Conference on Solid-State Sensors, Actuators and Microsystems & Eurosensors XXXIII*, pp. 1246–1249, 2019.
- [7] Y. Sasago *et al.*, “SiC-FET-type NO_x Sensor for High-Temperature Exhaust Gas,” *Technical Digest - International Electron Devices Meeting, IEDM*, pp. 12.5.1–12.5.4, 2018.
- [8] I. I. Soykal *et al.*, “Amperometric NO_x Sensor Based on Oxygen Reduction,” *IEEE Sensors Journal*, vol. 16, no. 6, pp. 1532–1540, 2016.
- [9] H. Wang *et al.*, “Structural and Properties Study of Li_3PO_4 Thin Film Electrolyte for Potentiometric Nox Sensing,” *2017 5th International Conference on Mechanical, Automotive and Materials Engineering, CMAME 2017*, pp. 23–27, 2018.
- [10] “On-board Emissions Measurement System OBS-one,” *Horiba Automotive Test Systems*. [Online]. Available: https://www.horiba.com/en_en/products/detail/action/show/Product/obs-one-gs-unit-28/
- [11] J. Eriksson and S. Fagerholm, “Exhaust Analyser for Simplified Emissions Testing on Heavy Duty Vehicles,” *Master Thesis, KTH Industrial Engineering & Management*, 2014.
- [12] NI, “cRIO 9057 Datasheet.” [Online]. Available: http://www.ni.com/pdf/manuals/377522b_02.pdf
- [13] R. W. Larsen, *LabVIEW for engineers*. Pearson Higher Ed, 2011.

- [14] M. Koebel *et al.*, “Urea-SCR: A promising technique to reduce NOx emissions from automotive diesel engines,” *Catalysis Today*, vol. 59, pp. 335–345, 2000.
- [15] I. Demirkiran *et al.*, “A Design to Improve Selective Catalytic Reduction for Diesel Engines,” *IEEE Southeast Conference 2016*, pp. 1–6, 2016.
- [16] J. M. Rheaume, “Solid State Electrochemical Sensors for Nitrogen Oxide (NOx) Detection in Lean Exhaust Gases,” *PhD Dissertation, University of California, Berkeley*, p. 164, 2010.
- [17] “Bosch CAN Specification,” *Robert Bosch GmbH*, 1991.
- [18] “Controller Area Network (CAN) Overview,” *National Instruments white paper*, 2019.
- [19] NI, “NI 9871 Datasheet.” [Online]. Available: <https://www.ni.com/en-us/support/model.ni-9871.html>
- [20] —, “NI 9845 Datasheet.” [Online]. Available: <https://www.ni.com/en-us/support/model.ni-9485.html>
- [21] —, “NI 9216 Datasheet.” [Online]. Available: <https://www.ni.com/en-us/support/model.ni-9216.html>
- [22] —, “NI 9220 Datasheet.” [Online]. Available: <https://www.ni.com/en-us/support/model.ni-9220.html>
- [23] —, “NI 9264 Datasheet.” [Online]. Available: <https://www.ni.com/en-us/support/model.ni-9264.html>
- [24] Xilinx, “7 Series FPGAs Datasheet,” 2020. [Online]. Available: https://www.xilinx.com/support/documentation/data_sheets/ds180_7Series_Overview.pdf
- [25] NI, “NI 9860 Datasheet.” [Online]. Available: <https://www.ni.com/en-us/support/model.ni-9860.html>
- [26] G. Alrheis, “Personal communication referring to NDA protected Scania documentation, Södertälje,” 2020.
- [27] NI, “NI 9757 Datasheet.” [Online]. Available: <https://www.ni.com/en-us/support/model.ni-9757.html>